JOURNAL OF WATER AND LAND DEVELOPMENT
e-ISSN 2083-4535
Polish Academy of Sciences (PAN) Institute of Technology and Life Sciences – National Research Institute (ITP – PIB)

JOURNAL OF WATER AND LAND DEVELOPMENT
DOI: 10.24425/jwld.2026.157833
2026, No. 68 (I–III): 171–185

Experimental investigation of water aeration efficiency in a pipe aerator filled with Białecki rings

Marek Kalenik*[1)], Dariusz Morawski[1)], Marek Chalecki[2)], Piotr Wichowski[1)], Adam Kiczko[1)], Krzysztof Chmielowski[3)], Kamil Świętochowski[4)], Joanna Gwoździej-Mazur[5)]

[1)] Warsaw University of Life Sciences – SGGW, Institute of Environmental Engineering, Department of Hydraulics, Water and Sanitary Engineering, Nowoursynowska St, 159, 02-776 Warsaw, Poland

[2)] Warsaw University of Life Science – SGGW, Institute of Civil Engineering, Department of Mechanics and Building Structures, Nowoursynowska St, 159, 02-776 Warsaw, Poland

[3)] University of Science and Technology in Krakow – AGH, Faculty of Drilling, Oil and Gas, Department of Gas Engineering, Adama Mickiewicza al., 30, 30-059 Kraków, Poland

[4)] Warsaw University of Technology, Faculty of Environmental Engineering, Department of Information Science and Environment Quality Research, Nowowiejska St, 20, 00-653 Warsaw, Poland

[5)] Bialystok University of Technology, Faculty of Civil Engineering and Environmental Sciences, Department of Water Supply and Sewage Systems, Wiejska St, 45E, Białystok, Poland

* Corresponding author

RECEIVED 04.02.2025 ACCEPTED 07.01.2026 AVAILABLE ONLINE 18.03.2026

Abstract: In the era of the climate crisis, the availability of drinking water is becoming a growing concern. In Poland and in the world, rivers and water reservoirs used for drinking water abstraction and treatment are increasingly drying up. Drought is forcing greater reliance on groundwater, which often requires aeration during treatment to enable the removal of dissolved iron and manganese compounds. Therefore, this article presents the results of tests on the effectiveness of groundwater aeration in a PVC pipe aerator packed with steel Białecki rings. The tested pipe aerator was made according to patent PL 235924 B1. The article presents a critical literature review, the research methodology, an evaluation of measurement accuracy, an analysis of groundwater aeration performance, as well as an assessment of energy efficiency (e_Q) of the investigated pipe aerator. A nomogram was developed for design purposes to determine the air flow rate (Q_a) required in the pipe aerator depending on the desired oxygen content dissolved in the water aerated in the PVC pipe aerator. The investigations showed that the lowest oxygen dissolution occurred at Q_a = 0.5 $m^3 \cdot h^{-1}$, and the highest at Q_a = 3.0 $m^3 \cdot h^{-1}$, both for the rings with diameters of 12 mm and 25 mm.

Keywords: air flow rate, dissolved oxygen content, pipe aerator, steel Białecki rings, underground water treatment, water aeration efficiency, water flow rate

INTRODUCTION

Mixing is a unit operation used to facilitate chemical reactions in multiphase or multicomponent dispersions in chemical processes. In recent decades, mixing equipment has developed rapidly for a wide range of process applications across the chemical, oil, gas, petrochemical, cosmetic, pharmaceutical, food, and construction industries (Revathi *et al.*, 2020; Meng *et al.*, 2021). Mixing is also widely applied in environmental engineering, including oxygenation of watercourses (Baylar, Unsal and Ozkan, 2010; Puri, Sihag and Thakur, 2023), water reservoirs (JianChao *et al.*, 2021), and lakes and fish ponds (Loyless and Malone, 1998; Sadatomi *et al.*,

2015; Liew *et al.*, 2020), removal of petroleum derivatives from groundwater (Li *et al.*, 2014), domestic sewage treatment (Suwartha *et al.*, 2020), and groundwater treatment for food purposes (Kalenik *et al.*, 2023).

Mixing hydrodynamics always involve energy consumption, which usually affects the efficiency of mixing equipment. The most efficient mixing device transfers the maximum kinetic energy of liquids being mixed while requiring minimal external power input. Fixed (static) mixers use the kinetic energy of flowing fluids to achieve mixing. Traditional static mixers are made with pipes fitted with internal screw-type metal baffles (Yuan, Cui and Lin, 2020; Talhaoui, Draoui and Youcefi, 2021), helicoids (Chang *et al.*, 2011), paddles (Putra *et al.*, 2019), orifices (Sadatomi *et al.*, 2012), balls (Kawahara *et al.*, 2009), or Białecki rings (Kalenik *et al.*, 2023). In the static mixers, multiphase mixing is achieved by redirecting liquid and gas flows. This is a passive mixing method devoid of an external energy source and moving parts. Compared to mechanical mixers, static mixers are more economical for mixing and dispersion, do not require complex design, and are easy to manufacture and operate (Yuan , Cui and Lin, 2020). Previous studies have shown (Talhaoui, Draoui and Youcefi, 2021) that static mixers are better suited for industrial applications and water treatment plants because mixing is rapid, mixing quality is high, and liquid and gas residence times are short. In addition, self-cleaning can occur during operation, limiting sediment deposition in the mixer (Kalenik and Morawski, 2013).

Levitsky *et al.* (2005) presented results of experimental studies on water oxygen saturation in an eject aerator, which efficiently disperses air oxygen by producing fine bubbles at relatively low air and water supply pressures. The authors showed that the ejector aerator can improve water oxygenation and reduce aeration costs compared to conventional aerators.

Hussain (2021) presented results of experimental studies on the effectiveness of mixing water with air, i.e. oxygenating water, in a static pipe mixer. This mixer consisted of a horizontal plexiglass pipe with an 80 mm diameter, fitted with static elements placed at equal distances. Measurements were made at water flow rates of 4.5–20 $m^3 \cdot h^{-1}$ and air flow rates 0.3–1.2 $m^3 \cdot h^{-1}$. The tests encompassed measurements of pressure difference, dissolved oxygen concentration in water, and the diameters of air bubbles formed during the water and air flow through the mixer. Measurements were taken for five types of static elements, such as baffles, plates, wheels, blades, and needles, placed in the pipe aerator.

Hussain (2021) reported that the largest pressure drops, and thus hydraulic losses, occurred in the pipe mixer with the static baffle-type elements. The dissolved oxygen concentration in the aerated water flowing out of the mixer with the static baffle-type elements was significantly higher compared to the other static elements tested. In addition, when the water and air flow rates increased in the pipe mixer with static baffle-type elements, diameters of air bubbles tended to decrease compared to those produced by the other static elements. The researcher attributed the higher oxygen levels dissolved to rapid bubble breakup on both sides of the static baffle-type elements, as these elements have a symmetrical geometry compared to the other static elements examined. The second contributing factor was the larger surface area available for air bubbles dispersion, as each of the static elements contained five evenly spaced holes. Hussain also reported that increasing dissolved oxygen was associated with decreasing bubble diameters, because smaller bubbles increase mass transfer between phases. Therefore, parameters such as water velocity and air flow rate in a pipe mixer with baffle-type elements affect the mass transfer coefficient.

Water oxygenation in water supply systems can be also achieved using microbubbles. Microbubbles are very small air bubbles with a diameter of less than a few hundred micrometers which increase the oxygen solubility in the surrounding water. Microbubble generators with various design solutions are used to produce these microbubbles.

Sadatomi *et al.* (2005) presented a new solution for a mixer design, i.e. a microbubble generator with a spherical body inside a pipe. In this microbubble generator, pressurised water is introduced into the pipe and flows around the spherical body in its core. During the water flow through the generator, the velocity of water around the spherical body, especially in the lower region, is higher than the velocity of water at the inlet of the generator, which reduces local water pressure. When the water pressure drops below atmospheric pressure, air is automatically drawn into the water stream through several small holes drilled in the pipe wall in the lower pressure region downstream of the body centre. Since the water flow in this area is very turbulent, the sucked air is therefore broken into a large number of microbubbles. The authors performed a number of different measurements and, for an improved version of the microbubble generator, obtained experimental data on the air suction velocity, the hydraulic pressure needed to introduce water into the generator, the efficiency of microbubble production, and changes in the content of oxygen dissolved after oxygenation as a function of water supply velocity. Based on these measurements, the researchers determined an optimal ratio of spherical body diameter to pipe diameter and showed that the new generator can generate microbubbles with lower energy consumption and oxygenate water efficiently.

The new microbubble generator developed by Sadatomi *et al.* (2005) has low power consumption, up to 40 W, compared to other designs available on the market. Therefore, the pump supplying water to the microbubble generator can be a low-power device powered by electricity produced, for example, by photovoltaic panels. Photovoltaic panels are already widely used in water supply systems to power water supply pumps (Świętochowski *et al.*, 2023).

Sadatomi *et al.* (2012) described the structure and operation principle of a multifluid mixer developed as a microbubble generator with an orifice and porous pipe, and presented its detailed hydraulic characteristics, practical applications, and research findings. In this article, the researchers analysed the rate of air microbubble production by the mixer, which was placed in a water tank at depths of up to 3.6 m, and the dissolution rates of oxygen from air and carbon dioxide in tap water at a temperature of 20°C. The authors of the article showed that, for this multifluid mixer design, both microbubble formation rate and oxygen dissolution rate in tap water can be predicted well using the proposed mathematical models.

Kawahara *et al.* (2009) presented characteristics of microbubble dissolution in tap water and seawater with air microbubbles generated by a multifluid mixer-type generator with a spherical body in a pipe. In the experiments, tap water and artificial seawater with salt concentrations of 1 and 3% (by

weight) were used to examine the influence of salinity on the solubility of oxygen microbubbles in seawater. The results showed that the air-bubble generation rate decreased as salt concentration increased, because the average air-bubble diameter decreased with increasing salinity due to reduced surface tension and suppressed bubble coalescence. In contrast, the volumetric mass transfer coefficient increased with increasing seawater salinity.

Methods of producing microbubbles for water oxygenation vary. One approach is to use a Venturi-tube-type microbubble generator (mixer). A key advantage of this design is that no compressor is needed to supply air, as the Venturi tube entrains air from the atmosphere. The aeration efficiency of the Venturi-tube-type aerator depends on its geometric parameters (Yadav, Kumar and Sarkar, 2019). However, the size of air bubbles generated by a Venturi tube is relatively larger than in other methods. Therefore, many researchers have improved the generators (mixers) through various design modifications to enhance water oxygenation efficiency.

Therefore, Kim *et al.* (2018) improved the efficiency of the Venturi-tube-type generator by installing a breaking disc. The researchers performed several experiments in which the distance between the breaking disc and the air suction nozzle was varied to evaluate its effect. The tests showed that after the installation of a breaking disc in the Venturi tube, a reverse flow was created by the resistance exerted by the breaking disc at the fluid. The liquid pressure caused by the reverse flow and the resistance exerted by the breaking disc was inversely proportional to the distance between the breaking disc and the air suction nozzle. Therefore, at smaller distances, the liquid pressure drop was lower. which reduced the amount of air sucked into the Venturi tube. The authors of the paper also showed that, when the mass transfer coefficient remained constant, the entrained air flow rate was the lowest at a disc-nozzle distance of 30 mm, and the oxygen saturation time was the shortest. At disc-nozzle distances of 40, 45 and 50 mm, oxygen saturation times were comparable but longer than those observed without the breaking disc, and the entrained air flow rates were similar. This was attributed to the disc being close to the air suction nozzle, where large air bubbles impinge on the disc and break into smaller bubbles, and thus increase the efficiency of water oxygenation.

Liew *et al.* (2020) presented results on the oxygenation efficiency of a modified microbubble generator (mixer). The mixer was modified by installing a porous pipe and a 10 mm orifice in the Venturi tube, with the aim of reducing hydraulic resistance (friction) and thereby minimising energy loss. The results showed a tendency for dissolved oxygen derived from entrained air to increase with increasing water flow velocity at a constant air flow rate. In contrast, at constant water flow velocity, increasing air flow rate tended to decrease the dissolved oxygen content. However, the energy-efficiency analysis showed that the modified mixer did not minimise energy losses compared to similar industrial solutions. Therefore, the authors suggested that the design based on a porous pipe and orifice mounted in the Venturi tube should be further improved, with emphasis on balancing the size of generated air bubbles and the air flow rate in order to achieve greater efficiency of water oxygenation while minimising energy loss.

Various aerator (mixer) designs available on the market can be used to oxygenate water in water treatment plants. One of such solutions is a packed pipe aerator developed under Polish patent PL 235924 B1 (Kalenik and Morawski, 2020). Its design is presented in detail by Kalenik *et al.* (2023), along with guidelines for determining the local resistance coefficient (z) for this type of packed pipe aerator.

In contrast, the available scientific and technical literature lacks information how to determine, for design purposes, the air flow rate (Q_a) required for a packed pipe aerator based on patent PL 235924 B1 (Kalenik and Morawski, 2020) to achieve the target dissolved oxygen concentration. Achieving the required oxygen level is necessary to convert dissolved iron compounds in groundwater into insoluble forms that precipitate in the form of sediment, which can then be retained on an iron-removal filter. Therefore, the present article analyses results on the oxygenation efficiency of a PVC pipe aerator packed with steel Białecki rings (Kalenik and Morawski, 2020) and presents nomograms to determine the required air flow rate (Q_a) as a function of the required dissolved oxygen concentration in the aerated water for a packed pipe aerator based on patent PL 235924 B1. The study investigated a PVC pipe aerator with an internal diameter of 101.6 mm, packed with steel Białecki rings of 12 mm and 25 mm diameter.

In the tests, steel Białecki rings with diameters of 12 mm and 25 mm were used beacuse these are the smallest ring diameters available on the market. Białecki rings are commonly used as packing in static liquid and gas mixers, as well as in pipe aerators employed in water treatment plants (Kalenik *et al.*, 2017). Steel Białecki rings are characterised by twofold lower hydraulic resistance than, for example, Raschig rings, and threefold higher throughput. They disperse liquid evenly across the column cross-section regardless of the feed method, maintain separation performance at a constant level regardless of the column hydraulic load, and have a rigid structure.

An additional rationale for using steel Białecki rings with diameters of 12 mm and 25 mm in the packed pipe aerator based on patent PL 235924 B1 (Kalenik and Morawski, 2020) is that previous investigations evaluated effectiveness of water aeration in pipe aerators using such packing (Kalenik and Morawski, 2013; Kalenik *et al.*, 2017). These studies reported higher effectiveness in pump aerators effectiveness than that obtained with other types of rings applied in pipe aerators (Siwiec and Morawski, 2000).

MATERIALS AND METHODS

DESCRIPTION OF THE MEASURING STAND

In order to test the effectiveness of water aeration in the packed pipe aerator, a measuring stand was built in the Scientific and Research Water Supply Station of the Warsaw University of Life Sciences; a diagram is shown in Figure 1. The pump (*1*) delivers water to the measuring stand through a pipeline (*2*). The supply pipeline (*2*) is equipped with an electromagnetic PROMAG 53P50 water flow meter (*3*) (Endress+Hauser) to measure water flow rate, and a needle valve (*4*) to precisely set the flow entering the pipe aerator (*6*). At the outlet of the pipe aerator (*6*), an impulse hose (*19*) is connected to an overflow tank (*23*).

The pipe aerator (*6*) was mounted vertically on the measuring stand. An air vent (*14*) was installed at the highest point of the stand. Air from the compressor (*8*) was supplied to the pipe aerator (*6*) through a pipeline (*9*) equipped with a needle valve (*10*) to precisely regulate the flow rate. Air flow rate was

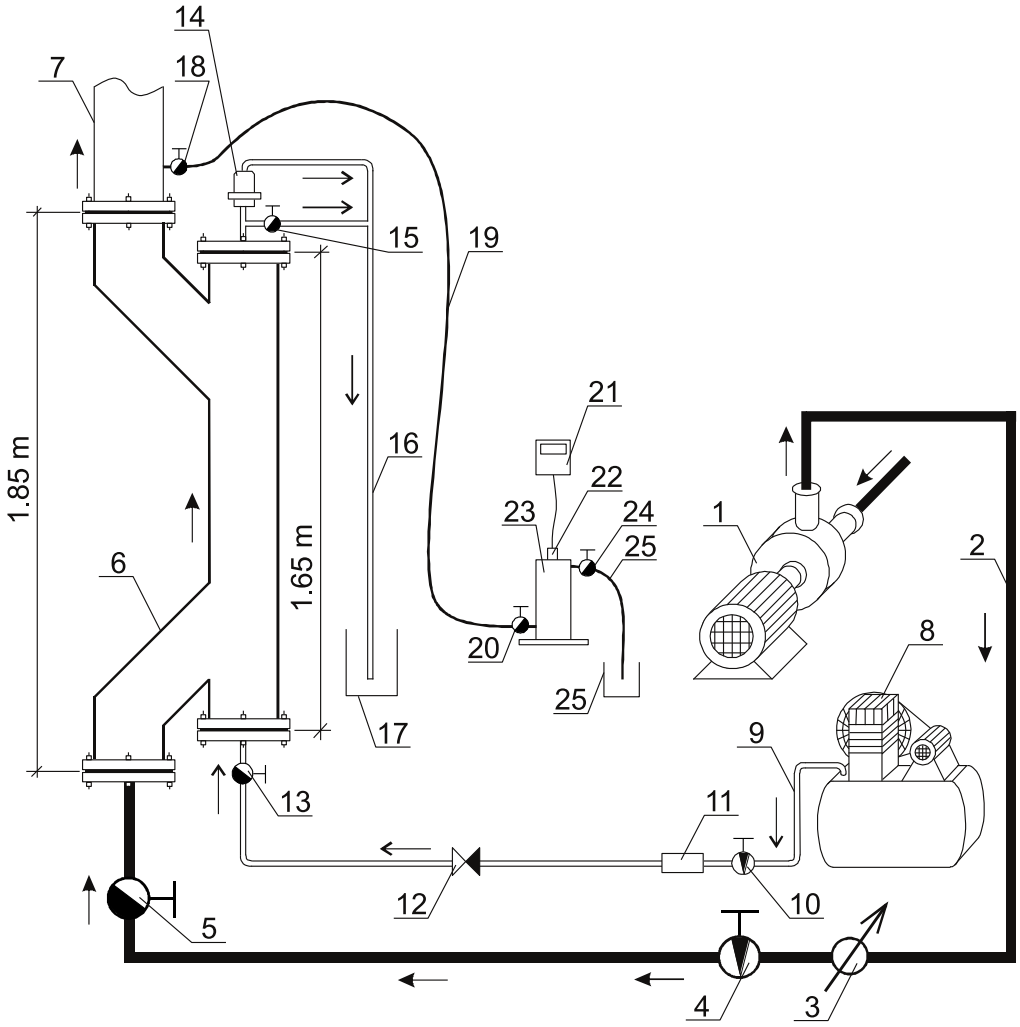

Fig. 1. Diagram of the measuring stand for testing the effectiveness of water aeration in a pipe aerator with filling: *1* = pump, *2* = water supply pipeline, *3* = electromagnetic water flow meter, *4* = needle valve for water flow control, *5*, *15*, *18*, *20*, *24* = ball valves cutting off the water flow, *6* = pipe aerator, *7* = water drainage pipeline, *8* = compressor, *9* = air supply pipeline, *10* = needle valve for air flow regulation, *11* = thermal air flow meter, *12* = non-return valve, *13* = ball valve cutting off the air flow, *14* = vent, *16* = pipe draining water and air to the sewerage, *17*, *25* = drain to the sewerage, *19* = aerated water supply hose, *21* = data logger with display, *22* = electrode for measuring water temperature and content of the oxygen dissolved in water, *23* = tank with overflow, *25* = hose for draining aerated water to sewerage; source: own elaboration

measured using a thermal flow meter (EE741; E+E Elektronik) (*11*), and a non-return valve (*12*) was installed on the air supply pipeline (*9*). Water temperature and dissolved oxygen in the aerated water were measured using a Hanna edge HI 2004-2 oxygen meter (Mera) equipped with a data logger with display (*21*) and a probe (*22*) for measuring dissolved oxygen and water temperature. The measuring stand operated as an open system, so water leaving the system was discharged into the sewer (*7*).

The electromagnetic flowmeter (*3*) has a measurement range of 0.0–70 $m^3 \cdot h^{-1}$, and the thermal air flowmeter (*11*) has a range of 0.0–75 $m^3 \cdot h^{-1}$. The measurement error of the electromagnetic water flow meter is below 2%, and that of the thermal air flow meter does not exceed 3%; the output current signal range is 4–20 mA. The dissolved oxygen probe has a measurement range of 0.0–45 $mg \cdot dm^{-3}$, a resolution of 0.01 $mg \cdot dm^{-3}$, and an accuracy of ±1.5%. The accuracy of the water temperature probe is ±0.2°C and a resolution of 0.1°C.

During dissolved oxygen tests, the pipe aerator (Photo 1) was packed with steel Białecki rings of 12 mm and 25 mm diameter. The packing height was 1 m. The pipe aerator used in the study had an internal diameter of 101.6 mm and a height of 1.85 m (Photo 1).

Photo 1. Steel Białecki rings: a) with the diameter 25 mm, b) with the diameter 12 mm (phot.: *M. Kalenik*)

METHOD OF INVESTIGATIONS

Measurements of dissolved oxygen in water aerated in the PVC pipe aerator were performed using steel Białecki rings with diameters 12 mm and 25 mm. Before each measurement series, it was verified that all valves on the measuring stand (Fig. 1) were closed. At the start of each measurement series, valves (*5*), (*13*), (*18*), (*20*), and (*25*) were opened. The pump (*1*), compressor (*8*), and the data logger (*21*) with the probe (*22*) for measuring water temperature and dissolved oxygen were switched on. After the system was filled with water, the initial water flow rate (Q_w) was set on the electromagnetic flow meter (*3*) using the needle valve (*4*), and the initial air flow rate (Q_a) was set on the thermal air flow meter (*11*) using the needle valve (*10*). Once water and air flow conditions stabilised, dissolved oxygen and water temperature (T) were read from the data logger (*21*). Then, the needle valve (*4*) was used to set the next Q_w value, and the needle valve (*10*) to set the next Q_a value. After flow conditions stabilised again, subsequent O_2 and T readings were recorded.

Dissolved oxygen measurements were carried out at water flow rates (Q_w) of 2–20 $m^3 \cdot h^{-1}$ in 2 $m^3 \cdot h^{-1}$ increments, and air flow rates (Q_a) of 0.5–3.0 $m^3 \cdot h^{-1}$ in 0.5 $m^3 \cdot h^{-1}$ increments. During the measurements, slight pulsations in Q_w due to pump operation and in Q_a due to compressor operation were observed on the electromagnetic flowmeter (*3*), which also affected the dissolved oxygen readings recorded by the data logger (*21*). In order to eliminate accidental measurement errors, three measurement series were performed for each Q_w and Q_a setting, and the results were averaged. In total, five averaged measurement series were made for each steel Białecki ring diameter.

Figure 2 presents a flowchart of the investigations and statistical analyses performed for the pipe aerator with the steel Białecki rings with the diameters 12 and 25 mm.

RESULTS AND DISCUSSION

Figure 3 presents dissolved oxygen concentrations measured in water aerated in the PVC pipe aerator packed with steel Białecki rings of 12 mm and 25 mm diameter, as a function of the set water flow rate (Q_w) and air flow rate (Q_a). During the measurements, dissolved oxygen decreased with increasing Q_w (Fig. 3), and increased with increasing Q_a, consistent with trends reported in the literature (Kalenik and Morawski, 2013; Kalenik *et al.*, 2017).

Analysis of Figure 3 indicates that, at the same set Q_w and Q_a, dissolved oxygen concentrations were higher in water aerated in the pipe aerator packed with steel Białecki rings of 12 mm diameter than in the pipe aerator packed with 25 mm rings. This is attributed to the higher hydraulic resistance in the pipe aerator packed with 12 mm rings compared to 25 mm rings (Kalenik *et al.*, 2023). Therefore, air bubbles remained in contact with water for a longer time in the 12 mm packing, resulting in greater oxygen dissolution in water.

Water temperature as well as the size of air bubbles also affects the amount of oxygen dissolved in water (Levitsky *et al.*, 2005; Sadatomi *et al.*, 2015; Hussain, 2021). Increasing water temperature reduces oxygen solubility and therefore decreases the rate of oxygen penetration into water. During the measurements, the temperature of the aerated water ranged from 12.0 to 12.7°C. In addition, smaller bubbles (microbubbles, micro-nanobubbles) provide larger interfacial area for gas-liquid contact, which enhances solubility of oxygen. Microbubbles and micro-nanobubbles implode violently in water, which can further accelerate oxygen dissolution (Kawahara *et al.*, 2009; Sadatomi *et al.*, 2012; Li *et al.*, 2014; Liew *et al.*, 2020). In the experiment, highly fragmented air bubbles were observed in the oxygenated water.

The tests showed (Fig. 3) that in the water aerated in the packed pipe aerator, the lowest oxygen solubility occurred at $Q_a = 0.5\ m^3 \cdot h^{-1}$, and the highest at $Q_a = 3\ m^3 \cdot h^{-1}$, both for 12 mm and 25 mm rings.

Based on the dissolved oxygen measurements (Fig. 3) obtained for water oxygenated in the PVC pipe aerator packed with steel Białecki rings of 12 mm and 25 mm diameter, measurement uncertainty for the mean dissolved oxygen was estimated according to Equation (1) (Oktaba, 1980):

$$\sigma_{\bar{x}} = \sqrt{\frac{\sum_{i=1}^{n} (x_i - \bar{x})^2}{n(n-1)}} \tag{1}$$

where: $\sigma_{\bar{x}}$ = measurement uncertainty (mg $O_2 \cdot dm^{-3}$), x_i = result of an i-th measurement (mg $O_2 \cdot dm^{-3}$), $\bar{x}$ = arithmetic mean of a series of n measurements (mg $O_2 \cdot dm^{-3}$), n = number of measurements (–).

The estimated average measurement uncertainties for dissolved oxygen in water oxygenated in the PVC pipe aerator packed with steel Białecki rings of 12 mm and 25 mm diameter are presented in Table 1.

Analysis of Table 1 indicates that the estimated mean uncertainties ($\sigma_{\bar{x}}$) of dissolved oxygen measurements were very small. After rounding to two significant digits, consistent with the resolution of the dissolved oxygen probe, the mean uncertainty was $\sigma_{\bar{x}} = \pm 0.01$ mg $O_2 \cdot dm^{-3}$. This indicates that the dissolved oxygen measurements were performed with high accuracy.

Table 2 presents the basic statistics of dissolved oxygen in water aerated in the PVC pipe aerator packed with steel Białecki rings of 12 mm and 25 mm diameter.

Analysis of Table 2 indicates that the diameter of the steel Białecki rings significantly affected the aeration efficiency in the packed pipe aerator. Therefore, using Equation (2), the reduction in aeration efficiency for water aerated in the PVC pipe aerator

Fig. 2. Flowchart of the investigations and statistical analyses performed for the pipe aerator with steel Białecki rings of 12 mm and 25 mm diameter: *1* = construction of the measuring rig, *2* = methodological development of the investigations, *3* = measurements, *4* = estimation of a measurement uncertainty, *5* = statistical analysis of measurements, *6* = determination of formulas for calculations oxygen content in water leaving the aerator, *7* = a statistical analysis for a verification of the correctness of the fitting of the logarithmic model for calculating the content of the oxygen dissolved in water leaving the aerator, *8* = development of a nomogram for reading the air flow rate related to the required content of the oxygen O_2 dissolved in the water leaving the aerator, *9* = determination of the energy efficiency coefficient for the investigated aerator; source: own elaboration

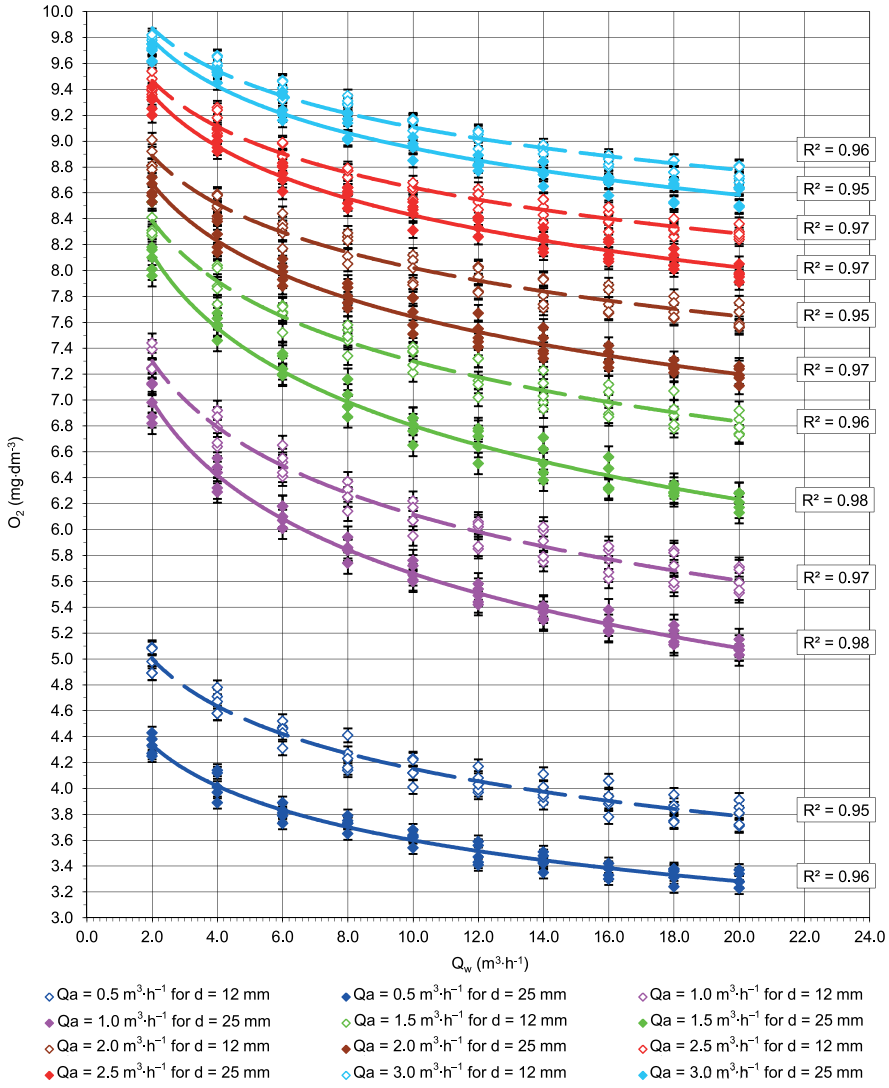

Fig. 3. Dependence of content of the oxygen (O_2) dissolved in water aerated in the PVC pipe aerator with steel Białecki rings with diameters d = 12 mm and d = 25 mm on water flow rate (Q_w) and air flow rate (Q_a); source: own study

Table 1. Average measurement uncertainties for dissolved oxygen (O_2) in water oxygenated in the PVC pipe aerator packed with steel Białecki rings of 12 mm and 25 mm diameter

Air flow rate Q_p ($m^3 \cdot h^{-1}$)	Diameter d (mm)	Measurement uncertainty $\sigma_{\bar{x}}$ (mg $O_2 \cdot dm^{-3}$)
0.5	12	±0.0073
	25	±0.0039
1.0	12	±0.0100
	25	±0.0058
1.5	12	±0.0101
	25	±0.0080
2.0	12	±0.0079
	25	±0.0071
2.5	12	±0.0040
	25	±0.0048
3.0	12	±0.0023
	25	±0.0045

Source: own study.

packed with steel Białecki rings of 25 mm diameter relative to 12 mm rings was calculated, and the results are presented in Table 3:

$$ZSNW = \frac{O_{2d12} - O_{2d25}}{O_{2d12}} 100\% \quad (2)$$

where: $ZSNW$ = water aeration efficiency reduction (%); O_{2d12} and O_{2d25} = content of the oxygen (mg·dm^{-3}) dissolved in water aerated in the PVC aerator with steel Białecki rings with diameters d = 12 mm and d = 25 mm, respectively.

Analysis of calculations in Table 3 indicates that, as the set air flow rate (Q_a) increased, the aeration efficiency reduction ($ZSNW$) for the water aerated in the PVC pipe aerator packed with the steel Białecki rings of 25 mm diameter relative to 12 mm rings became less pronounced. The $ZSNW$ values in Table 3 show that at Q_a = 0.5 $m^3 \cdot h^{-1}$, the mean oxygenation efficiency for 12 mm rings was 13.33% higher than that for 25 mm rings. In contrast, at Q_a = 3.0 $m^3 \cdot h^{-1}$, the mean oxygenation efficiency for 12 mm rings was only 1.75% higher than for 25 mm rings. Therefore, as Q_a increases, rings diameter has progressively smaller effect on water oxygenation efficiency in the packed pipe aerator.

Table 2. Basic statistics of the content of the oxygen (O_2) dissolved in the water aerated in the PVC pipe aerator pakced with steel Białecki rings of 12 mm and 25 mm diameter

Air flow rate Q_a ($m^3 \cdot h^{-1}$)	Diameter d (mm)	Content of the O_2 ($mg \cdot dm^{-3}$)			
		minimum	maximum	average	median
0.5	12	3.71	5.09	4.20	4.12
	25	3.23	4.43	3.64	3.58
1.0	12	5.51	7.44	6.19	6.05
	25	5.03	7.13	5.74	5.59
1.5	12	6.73	8.53	7.37	7.29
	25	6.13	8.18	6.88	6.76
2.0	12	7.56	9.01	8.07	7.98
	25	7.11	8.72	7.71	7.57
2.5	12	8.24	9.54	8.69	8.61
	25	7.91	9.42	8.48	8.41
3.0	12	8.68	9.82	9.15	9.08
	25	8.49	9.75	8.99	8.87

Source: own study.

Table 3. Reduction of the efficiency of water aeration (*ZSNW*) in the PVC pipe aerator with steel Białecki rings with diameter 25 mm compared to rings with diameter 12 mm

Air flow rate Q_a ($m^3 \cdot h^{-1}$)	*ZSNW* (%)			
	minimum	maximum	average	median
0.5	12.94	12.97	13.33	13.11
1.0	8.71	4.17	7.27	7.60
1.5	8.92	4.10	6.65	7.27
2.0	5.95	3.22	4.46	5.14
2.5	4.00	1.26	2.42	2.32
3.0	2.19	0.71	1.75	2.31

Source: own study.

A statistical analysis was also performed to determine whether differences in the mean dissolved oxygen values measured in the PVC pipe aerator packed with 12 mm and 25 mm steel Białecki rings (Fig. 3) were statistically significant. Firstly, a distribution normality was assessed using the Shapiro-Wilk test, followed by homogeneity of variance using Levene's test. The results are summarised in Table 4. For all groups, the calculated probability values (p_{cal}) exceeded the assumed significance level (α = 0.05), indicating that the date were normally distributed and that variances were homogeneous across the groups studied.

Student's *t*-test was then applied to compare the two populations. The null hypothesis assumed equal mean values (H_0: $n_1 = n_2$), whereas the alternative hypothesis assumed that the mean values differed (H_1: $n_1 \neq n_2$). The calculated values of the *t*-Student's statistic $|t_{cal}|$ are summarised in Table 5. To calculate the normality of distribution, uniformity of variance and Student's *t*-tests were performed using the Statistica software environment.

Table 4. Calculated values of oxygen dissolved in water according to the Shapiro-Wilk and Levene tests relative to the air flow rate (Q_a) for the 12 mm and 25 mm steel Białecki rings

Air flow rate Q_a ($m^3 \cdot h^{-1}$)	Diameter d (mm)	Probability value (p_{cal}) calculated with	
		Shapiro-Wilk test	Levene test
0.5	12	0.135470	0.139198
	25	0.144011	
1.0	12	0.149404	0.212635
	25	0.135826	
1.5	12	0.113422	0.320082
	25	0.129273	
2.0	12	0.125417	0.919850
	25	0.129773	
2.5	12	0.123046	0.472332
	25	0.106104	
3.0	12	0.134961	0.245191
	25	0.155261	

Note: differences in mean values are significant with probability $p > 0.05$.
Source: own study.

For the alternative hypothesis, the critical area was defined as $|t_{cal}| \geq t_{\alpha=0.05}$. Using *t*-Student's distribution tables (Oktaba, 1980), with $\nu = n_1 + n_2 - 2 = 98$ degrees of freedom and $\alpha = 0.05$ (i.e. 5% significance level), the critical value was $t_{\alpha=0.05} = 1.983$. As shown in Table 5, $|t_{cal}| \geq t_{\alpha=0.05}$; hence, the null hypothesis was rejected, and the differences between the mean dissolved oxygen values measured in the PVC pipe aerator packed with 12 mm and 25 mm steel Białecki rings were statistically significant. This conclusion is also supported by the calculated probability value, $p_{cal} < 0.05$ (assumed significance level).

In groundwater, iron occurs in a dissolved form. In order to remove iron from groundwater, water must be aerated in an aerator (mixer). During the aeration process, hydrolysis and oxidation reactions occur, as shown in Equations (3) and (4):

$$Fe(HCO_3)_2 + H_2O \rightarrow Fe(OH)_2 + 2CO_2 \quad (3)$$

$$2Fe(OH)_2 + 1/2O_2 + H_2O \rightarrow Fe(OH)_3 \quad (4)$$

This transforms iron present in water in a dissolved form into a poorly soluble form that precipitates as a sediment, which is then retained during filtration on the bed of a de-ironing filter. Depending on the iron content in groundwater, laboratory tests are used to determine the dissolved oxygen level needed for iron to convert from the dissolved form to the poorly soluble form. Therefore, to apply a PVC pipe aerator packed with steel Białecki rings of 12 mm and 25 mm diameter in a groundwater treatment plant, it is necessary to determine the required air flow rate (Q_a) for a given water flow rate (Q_w) and target dissolved oxygen concentration, so that hydrolysis and oxidation occur in the raw water and dissolved iron is converted to a poorly soluble form that precipitates and can be retained in the de-ironing filter. Therefore, using the dissolved oxygen measurement obtained in the PVC pipe aerator packed with 12 mm and 25 mm steel Białecki rings (Fig. 4) as a function of Q_w and Q_a, equations for

Table 5. Calculated dissolved oxygen in water according to the *t*-Student test relative to the air flow rate (Q_a) for the 12 mm and 25 mm steel Białecki rings

Air flow rate Q_a ($m^3 \cdot h^{-1}$)	Diameter d (mm)	Standard deviation	Value calculated from the *t*-Student test $\lvert t_{cal} \rvert$	Calculated probability value p_{cal}	Value of the *t*-Student test read from tables for $p = 0.05$, $v = 98$ $t_{a=0.05}$
0.5	12	0.380	35.400	0.000	1.983
	25	0.327			
1.0	12	0.527	22.148		
	25	0.587			
1.5	12	0.483	23.150		
	25	0.585			
2.0	12	0.388	25.172		
	25	0.457			
2.5	12	0.366	38.048		
	25	0.414			
3.0	12	0.341	36.817		
	25	0.375			

Note: differences in mean values are significant with probability $p < 0.05$.
Source: own study.

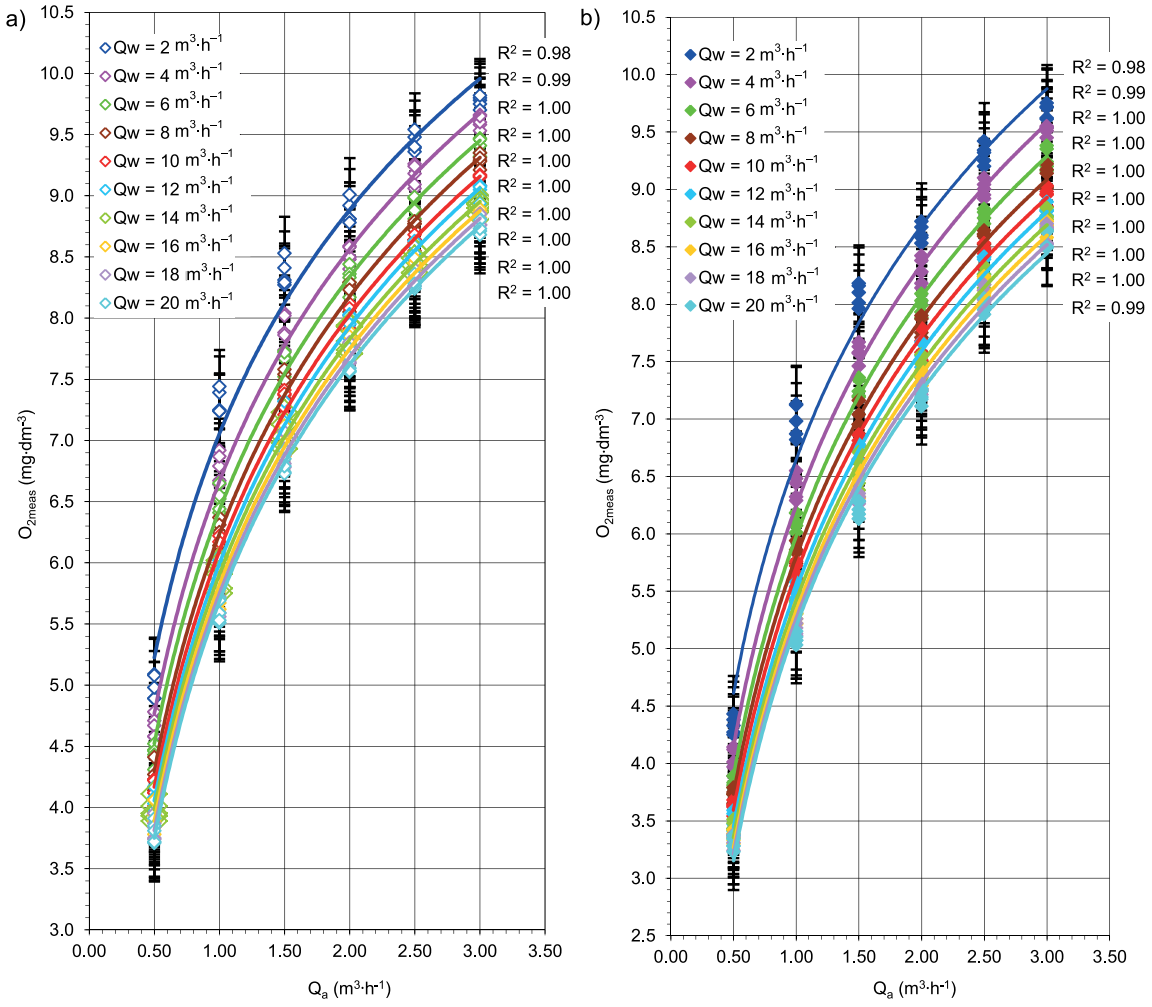

Fig. 4. Relation between the measured values of oxygen (O_{2meas}) dissolved in water aerated in a PVC pipe aerator packed with steel Białecki rings: a) 12 mm, b) 25 mm and the water flow rate (Q_a); source: own study

calculating dissolved oxygen in water aerated in the packed pipe aerator were determined and presented in Table 6. The fitted trend (regression) for the measured dissolved oxygen values (O_{2meas}) was logarithmic (Fig. 4). The sample determination coefficients (R^2) were above 0.98, indicating that dissolved oxygen in water aerated in the packed pipe aerator depends in 98% on Q_a and Q_w, and ring diameter, and in 2% on other factors, such as temperature, surface tension, and viscosity of the water and the fragmentation of air bubbles.

The fit of the logarithmic mathematical model to calculate the content of the oxygen dissolved in the water aerated in the PVC pipe aerator with steel Białecki rings (diameters 12 mm and 25 mm) was assessed using the graph in Figure 5. The values (Q_{2meas}) obtained from the measurements (Fig. 4) were placed on the vertical axis, while the results obtained from calculations using the equations in Table 6, i.e. the predicted values of O_{2calc}, were plotted on the horizontal axis. The data points were approximated by a linear function passing through the origin of the coordinate system; therefore the value of the directional coefficient of this linear function served to verify the correctness of the mathematical model. Analysing the relationship shown in

Table 6. Summary of the determined equations for calculating the content of the oxygen O_{2calc} dissolved in the water aerated in a PVC pipe aerator with steel Białecki rings packed with 12 mm and 25 mm rings relative to the water flow rate (Q_w)

Water flow rate Q_w ($m^3 \cdot h^{-1}$)	Determined Equations	No of Equation
d = 12 mm		
2	$O_{2calc} = 2.64 \cdot \ln(Q_a) + 7.06$	(5)
4	$O_{2calc} = 2.74 \cdot \ln(Q_a) + 6.67$	(6)
6	$O_{2calc} = 2.75 \cdot \ln(Q_a) + 6.43$	(7)
8	$O_{2calc} = 2.80 \cdot \ln(Q_a) + 6.24$	(8)
10	$O_{2calc} = 2.79 \cdot \ln(Q_a) + 6.10$	(9)
12	$O_{2calc} = 2.80 \cdot \ln(Q_a) + 5.99$	(10)
14	$O_{2calc} = 2.77 \cdot \ln(Q_a) + 5.91$	(11)
16	$O_{2calc} = 2.78 \cdot \ln(Q_a) + 5.82$	(12)
18	$O_{2calc} = 2.79 \cdot \ln(Q_a) + 5.75$	(13)
20	$O_{2calc} = 2.79 \cdot \ln(Q_a) + 5.69$	(14)
d = 25 mm		
2	$O_{2calc} = 2.94 \cdot \ln(Q_a) + 6.65$	(15)
4	$O_{2calc} = 3.03 \cdot \ln(Q_a) + 6.25$	(16)
6	$O_{2calc} = 3.01 \cdot \ln(Q_a) + 5.98$	(17)
8	$O_{2calc} = 2.99 \cdot \ln(Q_a) + 5.80$	(18)
10	$O_{2calc} = 2.98 \cdot \ln(Q_a) + 5.66$	(19)
12	$O_{2calc} = 2.99 \cdot \ln(Q_a) + 5.52$	(20)
14	$O_{2calc} = 2.98 \cdot \ln(Q_a) + 5.42$	(21)
16	$O_{2calc} = 2.97 \cdot \ln(Q_a) + 5.33$	(22)
18	$O_{2calc} = 2.96 \cdot \ln(Q_a) + 5.26$	(23)
20	$O_{2calc} = 2.95 \cdot \ln(Q_a) + 5.20$	(24)

Source: own study.

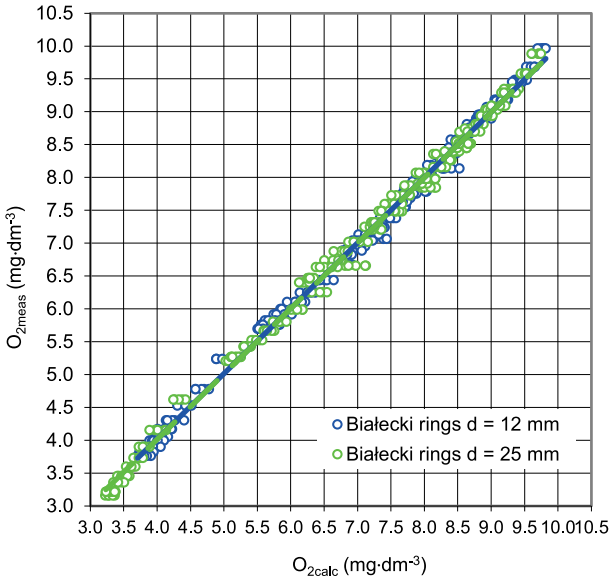

Fig. 5. Verification of the correctness of the fitting of the logarithmic model for calculating the content of the oxygen dissolved in water aerated in the aerator with steel Białecki rings with the diameters 12 and 25 mm; source: own study

Figure 5 indicates good concordance with the logarithmic mathematical model, because the directional coefficient of the linear function was 1 for both ring diameters (12 mm, 25 mm).

Table 7 presents the basic statistics regarding the content of oxygen dissolved in water aerated in the PVC pipe aerator packed

Table 7. Basic statistics of the content of the oxygen dissolved in the water aerated in the PVC pipe aerator packed with steel Białecki rings of 12 mm and 25 mm diameters, for the measured values O_{2meas} and calculated values O_{2calc} with relation to the water flow rate (Q_w)

Parameter	Water flow rate Q_w ($m^3 \cdot h^{-1}$)	Content of O_2 ($mg \cdot dm^{-3}$)			
		minimum	maximum	average	median
d = 12 mm					
O_{2meas}	2	4.89	9.82	8.12	8.65
O_{2calc}		5.23	9.96	8.12	8.51
O_{2meas}	4	4.58	9.66	7.77	8.22
O_{2calc}		4.77	9.68	7.77	8.18
O_{2meas}	6	4.31	9.47	7.54	7.95
O_{2calc}		4.52	9.45	7.54	7.94
O_{2meas}	8	4.14	9.35	7.37	7.815
O_{2calc}		4.30	9.32	7.37	7.79
O_{2meas}	10	4.01	9.17	7.22	7.65
O_{2calc}		4,17	9.17	7.22	7.63
O_{2meas}	12	3.97	9.08	7.12	7.58
O_{2calc}		4.05	9.07	7.12	7.53
O_{2meas}	14	3.89	8.97	7.03	7.47
O_{2calc}		3.99	8.95	7.03	7.43

cont. Tab. 7

Parameter	Water flow rate Q_w ($m^3 \cdot h^{-1}$)	Content of O_2 ($mg \cdot dm^{-3}$)			
		minimum	maximum	average	median
O_{2meas}	16	3.78	8.89	6.94	7.40
O_{2calc}		3.89	8.87	6.94	7.35
O_{2meas}	18	3.74	8.85	6.88	7.35
O_{2calc}		3.82	8.82	6.88	7.28
O_{2meas}	20	3.71	8.81	6.81	7.24
O_{2calc}		3.76	8.76	6.81	7.22
d = 25 mm					
O_{2meas}	2	4.25	9.75	7.83	8.36
O_{2calc}		4.61	9.88	7.83	8.26
O_{2meas}	4	3.89	9.55	7.47	7.91
O_{2calc}		4.15	9.58	7.47	7.91
O_{2meas}	6	3.73	9.38	7.19	7.62
O_{2calc}		3.89	9.29	7.19	7.63
O_{2meas}	8	3.65	9.22	7.01	7.44
O_{2calc}		3.73	9.08	7.01	7.44
O_{2meas}	10	3.54	9.03	6.86	7.19
O_{2calc}		3.59	8.93	6.86	7.30
O_{2meas}	12	3.41	8.89	6.73	7.10
O_{2calc}		3.48	8.81	6.73	7.16
O_{2meas}	14	3.35	8.84	6.62	7.02
O_{2calc}		3.35	8.69	6.62	7.06
O_{2meas}	16	3.30	8.72	6.53	6.91
O_{2calc}		3.27	8.59	6.53	6.96
O_{2meas}	18	3.24	8.70	6.45	6.78
O_{2calc}		3.21	8.51	6.45	6.89
O_{2meas}	20	3.23	8.64	6.39	6.70
O_{2calc}		3.16	8.44	6.39	6.82

Source: own study.

with steel Białecki rings of 12 mm and 25 mm diameters, both for the measured values O_{2meas} (Fig. 4) and calculated values O_{2calc} according to the determined equations 5–24 (Tab. 6), in relation to the water flow rate (Q_w).

Comparing the average values dissolved oxygen in water, measured O_{2meas} and calculated O_{2calc}, in relation to the flow rate of water (Q_w) aerated in the PVC pipe aerator with steel Białecki rings of 12 mm and 25 mm diameter (Tab. 7), it can be stated that they are identical, i.e. $O_{2meas} = O_{2calc}$.

A statistical analysis was also carried out to check whether the differences between the mean values of the measured content of oxygen dissolved in water (Fig. 4) and those calculated using equations 5–24 (Tab. 6) are statistically significant. Firstly, a distribution normality was assessed using the Shapiro-Wilk test, and then the uniformity of variance – using Levene's test. In both tests, for individual groups, the calculated probability values (p_{cal}) were higher than the assumed significance level $\alpha = 0.05$, indicating that the assumptions of normality and homogeneity of variance in the studied groups were met (Tab. 8). Student's t-test was then applied to the two populations, assuming the null hypothesis that the mean values are statistically equal (H_0: $n_1 = n_2$) and the alternative hypothesis (H_1: $n_1 \neq n_2$) that the mean values differ. The calculate values of the t-Student's statistic $|t_{cal}|$ are summarised in Table 9. The Statistica computer environment was used to calculate the normality of distributions, uniformity of variance, and Student's t-test.

Table 8. Results of calculations of the statistics of the content of the oxygen dissolved in water according to the Shapiro-Wilk and Levene test, for the measured values O_{2meas} and calculated values O_{2calc}, with relation to the water flow rate (Q_w) for the steel Białecki rings of d = 12 mm and d = 25 mm diameter

Parameter	Water flow rate Q_w ($m^3 \cdot h^{-1}$)	Probability value (p_{cal}) calculated with	
		Shapiro-Wilk test	Levene test
d = 12 mm			
O_{2meas}	2	0.159189	0.984021
O_{2calc}		0.181162	
O_{2meas}	4	0.202727	0.997675
O_{2calc}		0.181162	
O_{2meas}	6	0.163657	0.989913
O_{2calc}		0.181162	
O_{2meas}	8	0.160426	0.964289
O_{2calc}		0.181162	
O_{2meas}	10	0.163645	0.970303
O_{2calc}		0.181162	
O_{2meas}	12	0.159660	0.949266
O_{2calc}		0.181162	
O_{2meas}	14	0.155712	0.942658
O_{2calc}		0.181162	
O_{2meas}	16	0.164082	0.917726
O_{2calc}		0.181162	
O_{2meas}	18	0.169705	0.934262
O_{2calc}		0.181162	
O_{2meas}	20	0.168113	0.924489
O_{2calc}		0.181162	
d = 25 mm			
O_{2meas}	2	0.194136	0.943967
O_{2calc}		0.181162	
O_{2meas}	4	0.164458	0.957477
O_{2calc}		0.181162	
O_{2meas}	6	0.165520	0.960110
O_{2calc}		0.181162	
O_{2meas}	8	0.148417	0.989485
O_{2calc}		0.181162	

cont. Tab. 8

Parameter	Water flow rate Q_w ($m^3 \cdot h^{-1}$)	Probability value (p_{cal}) calculated with	
		Shapiro-Wilk test	Levene test
O_{2meas}	10	0.138832	0.972146
O_{2calc}		0.181162	
O_{2meas}	12	0.144659	0.955542
O_{2calc}		0.181162	
O_{2meas}	14	0.148440	0.914979
O_{2calc}		0.181162	
O_{2meas}	16	0.152551	0.889273
O_{2calc}		0.181162	
O_{2meas}	18	0.159367	0.869841
O_{2calc}		0.181162	
O_{2meas}	20	0.153532	0.846322
O_{2calc}		0.181162	

Note: differences in mean values are significant with probability $p > 0.05$.
Source: own study.

The Student's t-test was then applied to the two populations, assuming the null hypothesis that the mean values are statistically equal (H_0: $n_1 = n_2$) and an alternative hypothesis (H_1: $n_1 \neq n_2$) that the mean values differ. The calculated values of the t-Student's statistic $|t_{cal}|$ are summarised in Table 9. The Statistica computer environment was used to calculate the normality of distributions, uniformity of variance, and to perform Student's t-test.

Next, for the alternative hypothesis, the critical area $|t_{cal}| \geq t_{\alpha=0.05}$ was determined and, using the t-Student's distribution tables (Oktaba, 1980), for $\nu = n_1 + n_2 - 2 = 98$ degrees of freedom and $\alpha = 0.05$, i.e. the assumed 5% risk of error (significance level), the critical value $t_{\alpha=0.05} = 1.983$ was obtained. Analysis of Table 9 shows that $|t_{cal}| < t_{\alpha=0.05}$; hence, the null hypothesis cannot be rejected. It must be concluded that the differences between the mean values of the measured content of the oxygen dissolved and those calculated using equations 5–24 (Tab. 6) are not statistically significant. This conclusion is also confirmed by the calculated probability value, i.e. $p_{cal} > 0.05$ (the assumed significance level).

Therefore, taking into account Figure 5, which verifies the correctness of fitting the logarithmic model for calculating the dissolved oxygen content in water aerated in a pipe aerator with packing, as well as the results of statistical calculations using

Table 9. Results of calculations of the statistics of the content of the oxygen dissolved in water according to the t-Student test, for the measured values O_{2meas} and calculated values O_{2calc}, with relation to the water flow rate (Q_w) for the steel Białecki rings of d = 12 and d = 25 mm diameter

Parameter	Water flow rate Q_w ($m^3 \cdot h^{-1}$)	Standard deviation	Value calculated from the t-Student test $\|t_{cal}\|$	Calculated probability value p_{cal}	Value of the t-Student test read from tables for $p = 0.05$, $\nu = 98$ $t_{a=0.05}$ (Oktaba, 1980)
d = 12 mm					
O_{2meas}	2	1.638	–0.086	0.932	1.983
O_{2calc}		1.624			
O_{2meas}	4	1.689	–0.158	0.876	
O_{2calc}		1.686			
O_{2meas}	6	1.696	0.085	0.933	
O_{2calc}		1.692			
O_{2meas}	8	1.726	–0.140	0.889	
O_{2calc}		1.723			
O_{2meas}	10	1.716	–0.155	0.878	
O_{2calc}		1.715			
O_{2meas}	12	1.722	0.113	0.911	
O_{2calc}		1.723			
O_{2meas}	14	1.709	–0.145	0.886	
O_{2calc}		1.704			
O_{2meas}	16	1.715	0.114	0.909	
O_{2calc}		1.710			
O_{2meas}	18	1.719	–0.031	0.976	
O_{2calc}		1.716			
O_{2meas}	20	1.719	–0.189	0.851	
O_{2calc}		1.716			

cont. Tab. 9

Parameter	Water flow rate Q_w ($m^3 \cdot h^{-1}$)	Standard deviation	Value calculated from the *t*-Student test $\lvert t_{cal} \rvert$	Calculated probability value p_{cal}	Value of the *t*-Student test read from tables for $p = 0.05$, $\nu = 98$ $t_{a=0.05}$ (Oktaba, 1980)
d = 25 mm					
O_{2meas}	2	1.824	–0.038	0.970	1.983
O_{2calc}		1.809			
O_{2meas}	4	1.867	–0.080	0.937	
O_{2calc}		1.864			
O_{2meas}	6	1.855	0.057	0.955	
O_{2calc}		1.852			
O_{2meas}	8	1.839	0.189	0.852	
O_{2calc}		1.839			
O_{2meas}	10	1.834	–0.228	0.821	
O_{2calc}		1.833			
O_{2meas}	12	1.842	0.029	0.977	
O_{2calc}		1.839			
O_{2meas}	14	1.835	–0.073	0.942	
O_{2calc}		1.833			
O_{2meas}	16	1.834	0.121	0.904	
O_{2calc}		1.827			
O_{2meas}	18	1.827	0.248	0.806	
O_{2calc}		1.821			
O_{2meas}	20	1.822	0.026	0.979	
O_{2calc}		1.815			

Note: differences in mean values are significant with probability $p < 0.05$.
Source: own study.

Student's t-test (Tab. 9), Equations (5–24) (Tab. 6) can be used to determine the dissolved oxygen content in water aerated in the PVC pipe aerator with steel Białecki rings of 12 mm and 25 mm diameter for the design of a groundwater treatment plant. Based on Equations (5–24), a nomogram was developed for design purposes to determine the air flow rate (Q_a) as a function of the required dissolved oxygen content in water aerated in the PVC pipe aerator with the internal diameter of 101.6 mm and steel Białecki rings of 12 mm and 25 mm diameter (Fig. 6).

During the tests of water aeration using the pipe aerator with Białecki rings, readings were also taken from the electricity meter to measure energy used by the submersible pump and the compressor. Therefore, the energy efficiency factor of the tested pipe aerator was determined using Equation (5):

$$e_Q = \frac{E}{V} \tag{5}$$

where: e_Q = energy efficiency factor ($kWh \cdot m^{-3}$), E = amount of electricity consumed by the submersible pump and compressor within a certain time range (kWh), V = volume of medium pumped within the same time range (m^3).

Figure 7 shows the energy efficiency factor (e_Q) of the PVC pipe aerator (internal diameter 101.6 mm) fitted with steel Białecki rings (12 mm and 25 mm diameter) as a function of water (Q_w) and air (Q_a) flow rates, determined using Equation (25).

Analysis of Figure 7 indicates that the energy efficiency ratio (e_Q) of the tubular aerator with steel Białecki rings decreases as the water (Q_w) and air (Q_a) flow rates increase. As a low water flow rate (Q_w = 2 $m^3 \cdot h^{-1}$), the energy efficiency ratio for individual air flow rates ranges from 3.19 $kWh \cdot m^{-3}$ at Q_a = 0.5 $m^3 \cdot h^{-1}$ to 1.60 $kWh \cdot m^{-3}$ at Q_a = 3.0 $m^3 \cdot h^{-1}$. As the water flow increases, the differences in the energy efficiency ratio among the air flow rates steadily decreases. At a high water flow rate (Q_w = 20 $m^3 \cdot h^{-1}$), the energy efficiency ratio varies slightly, from 0.43 $kWh \cdot m^{-3}$ at Q_a = 0.5 $m^3 \cdot h^{-1}$ to 0.38 $kWh \cdot m^{-3}$ at Q_a = 3.0 $m^3 \cdot h^{-1}$.

By comparing the energy efficiency factor (e_Q) of the pipe aerator with steel Białecki rings (Fig. 7) with the dissolved oxygen content in water aerated in the PVC pipe aerator (Fig. 3), it can be stated that low energy efficiency values were obtained when the dissolved oxygen was high, whereas high energy efficiency values corresponded to low dissolved oxygen content. This indicates that the energy efficiency factor (e_Q) of the pipe aerator with steel Białecki rings is inversely proportional to the dissolved oxygen content in the water aerated in this pipe aerator.

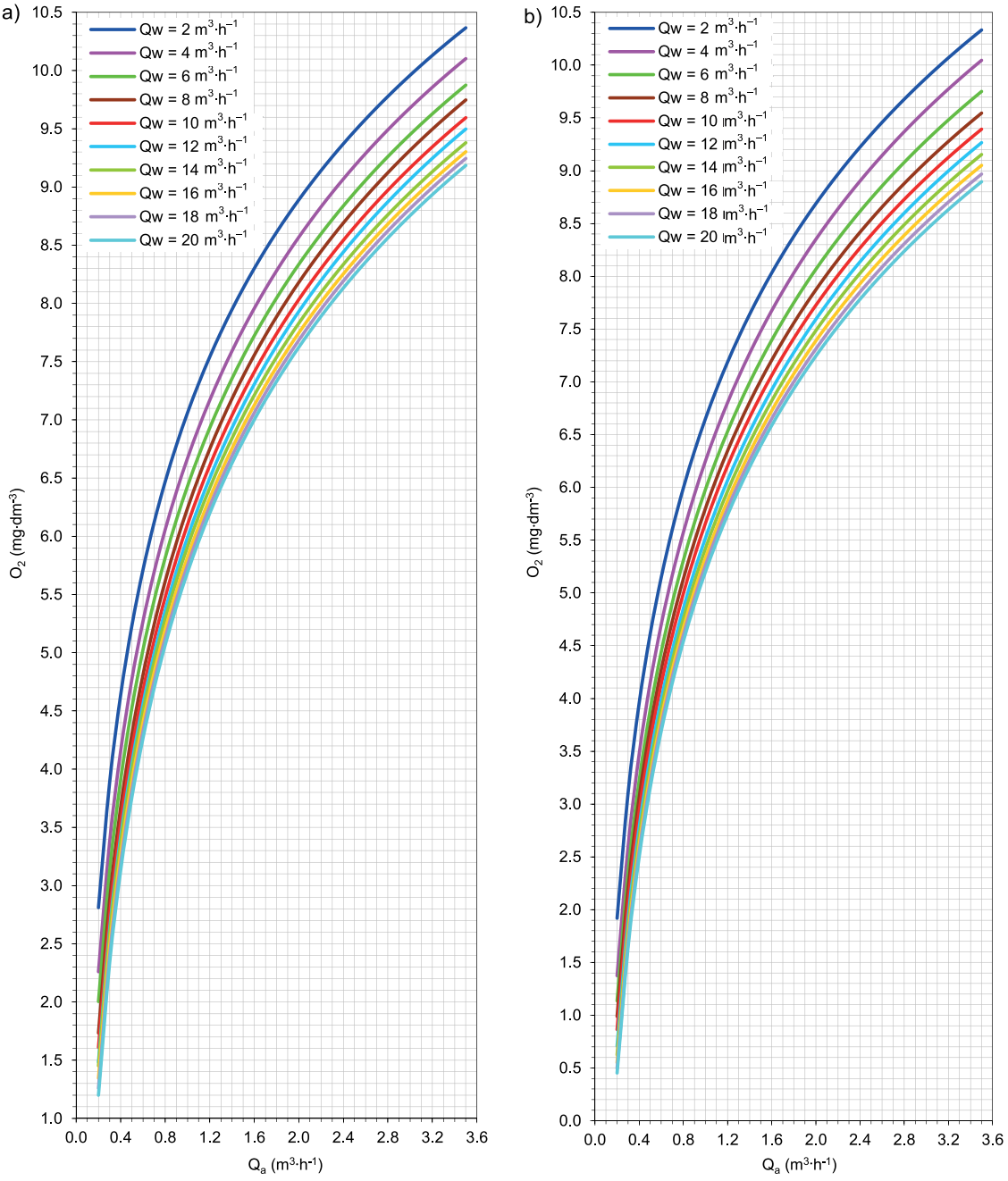

Fig. 6. Nomogram for reading the air flow rate (Q_a) related to the required content of the oxygen (O_2) dissolved in the water aerated in the PVC pipe aerator with the internal diameter 101.6 mm and steel Białecki rings with the diameters: a) d = 12 mm, b) d = 25 mm; source: own study

The pipe aerator with filling according to patent PL 235924 B1 (Kalenik and Morawski, 2020) is inexpensive to build and, compared to classic aerators, occupies little space in a water treatment plant. It is also easy to operate and environmentally safe, as it does not require any chemicals to oxidise the water, but only a small amount of air supplied by a compressor. Pipe aerators of this type are particularly suitable for containerised water treatment plants because of their compact size. From an economic point of view, building a containerised water treatment plant with filled pipe aerators according to patent PL 235924 B1 (Kalenik and Morawski, 2020) will be much cheaper than building a water treatment plant built in a concrete or brick structure.

To oxygenate water, potassium permanganate ($KMnO_4$) is often used because of its strong oxidising properties. In Poland, the current price of potassium permanganate is 61.34 PLN (gross) per 1 kg, and the price of electrical energy is ca. 0.62 PLN (gross) per 1 kWh. Therefore, it can be concluded that the pipe aerator with filling according to patent PL 235924 B1 (Kalenik and Morawski, 2020) will be cheaper to operate than aerators in which potassium permanganate is used.

The application of the nomogram (Fig. 7) is limited. It can only be used for pipe aerators with filling according to patent PL 235924 B1 (Kalenik and Morawski, 2020) and for cases in which the water flow rate does not exceed 20 $m^3 \cdot h^{-1}$. Because the flow capacity of a pipe aerator is limited by its diameter, increasing the

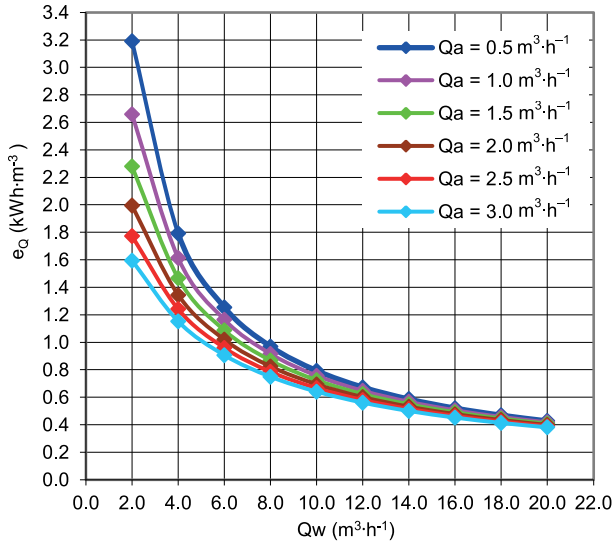

Fig. 7. Characteristics of the energy efficiency factor (e_Q) of the PVC pipe aerator with the internal diameter 101.6 mm and steel Białecki rings of 12 mm and 25 mm diameter as a function of water (Q_w) and air (Q_a) flow rates; source: own study

water flow rate through the aerator increases the water velocity and reduces the air-water contact time, which in turn deteriorates the aeration efficiency. Therefore, the water flow rate cannot be increased above the assumed value of 20 $m^3 \cdot h^{-1}$. This type of aerator must be filled with steel Białecki rings of 12 mm and 25 mm diameter, and their bulk thickness must not exceed 1 m. The pipe aerator must be constructed from polyvinyl chloride (PVC) pressure pipes (PVC-U PN 10) for bonded systems, with an outer diameter of 110 mm (inner diameter 101.6 mm), and must have a height of 1.85 m.

Therefore, further research is needed to develop nomograms for determining the required air flow rate Q_a as a function of the required dissolved oxygen content in water aerated in pipe aerators constructed according to patent PL 235924 B1, with external diameters greater than 110 mm. These aerators should be made of standard PVC pressure pipes (PVC-U PN 10) for potable water, for glued systems, generally available on the market, and filled with Białecki rings made of stainless steel or plastic.

CONCLUSIONS

1. The dissolved oxygen content in the water aerated in pipe aerators with steel Białecki rings is not constant and depends on the ring diameter, air flow rate (Q_a), and the water flow rate (Q_w). The developed nomogram with energy efficiency factor (e_Q) can be used in the design of groundwater treatment plants to determine the air flow rate required to achieve a desired dissolved oxygen content in water aerated in a PVC pipe aerator with an internal diameter of 101.6 mm and steel Białecki rings of 12 mm and 25 mm diameter.
2. The tests have shown very high water aeration efficiency in the pipe aerator with steel Białecki rings. As the ring diameter decreases and the air flow rate (Q_a) increases the dissolved oxygen content in the aerated water increases. In contrast, as the water flow rate (Q_w) increases, the dissolved oxygen content in the aerated water decreases.
3. The investigations showed that using 12 mm rings in the pipe aerator resulted in higher aeration efficiency due to a prolonged air-water contact. In contrast, when 25 mm rings were used, the aeration efficiency was lower because the contact time was shorter. Therefore, the air-water contact, and thus the aeration efficiency, can be adjusted by selecting ring diameters in the pipe aerator.
4. The energy efficiency factor (e_Q) of the pipe aerator with steel Białecki rings decreases as the water flow rate (Q_w) and the air flow rate (Q_a) increase, and it is inversely proportional to the dissolved oxygen content in the water aerated in the pipe aerator.
5. The pipe aerator with filling according to patent PL 235924 B1, using steel Białecki rings as the packing, is environmentally safe as it does not require any chemicals to oxidise the water, but only a small amount of air supplied by a compressor. From an economic point of view, it is inexpensive to construct and operate compared with traditional aerators.

CONFLICT OF INTERESTS

All authors declare that they have no conflict of interest.

REFERENCES

Baylar, A., Unsal, M. and Ozkan, F. (2010) "Hydraulic structures in water aeration processes," *Water, Air, & Soil Pollution*, 210, pp. 87–100. Available at: https://doi.org/10.1007/s11270-009-0226-2.

Chang, K.-T. *et al.* (2011) "Experimental and numerical study on the flow visualization in a tri-helical static mixer," *Journal of Marine Science and Technology*, 19(4), pp. 392–397. Available at: https://doi.org/10.51400/2709-6998.2180.

Hussain, M. (2021) "Comparison of different hydrodynamic characteristics of air-water system using dissimilar motionless mixers," *Sir Syed University Research Journal of Engineering & Technology*, 11(2), pp. 1–6. Available at: https://doi.org/10.33317/ssurj.228.

JianChao, S. *et al.* (2021) "Constraining release of pollutants from anoxic bottom sediment via water-lifting aeration in a source water reservoir, East China," *Journal of Soils and Sediments*, 21, pp. 3300–3309. Available at: https://doi.org/10.1007/s11368-021-02963-6.

Kalenik, M. *et al.* (2017) "Kinetics of water oxygenation in pipe aerator," *Infrastructure and Ecology of Rural Areas*, 2(2), pp. 689–700. Available at: https://dx.medra.org/10.14597/infraeco.2017.2.2.052.

Kalenik, M. *et al.* (2023) "Real values of local resistance coefficients during water flow through a pipe aerator with filling," *Journal of Water and Land Development*, 59, pp. 174–182. Available at: https://doi.org/10.24425/jwld.2023.147242.

Kalenik, M. and Morawski, D. (2013) "Eksperymentalne badania mętności i skuteczności napowietrzania wody w aeratorze rurowym wypełnionym pierścieniami Białeckiego [The experimental research on the turbidity and effectiveness of aerating water in pipe aerator with the Białecki rings]," *Infrastruktura i Ekologia Terenów Wiejskich*, 3(4), 217–227.

Kalenik, M. and Morawski, D. (2020) *Aerator rurowy z wypełnieniem [Pipe aerator with filling]*. Urząd Patentowy Rzeczypospolitej Polskiej. Opis patentowy nr PL 235924 B1. June 25, 2020.

Kim, H.-S. *et al.* (2018) "Effects of distance of breaker disk on performance of ejector type microbubble generator," *Journal of Civil Engineering*, 22(4), pp. 1096–1100. Available at: https://doi.org/10.1007/s12205-017-0208-7.

Kawahara, A. *et al.* (2009) "Prediction of micro-bubble dissolution characteristics in water and seawater," *Experimental Thermal and Fluid Science*, 33, pp. 883–894. Available at: https://doi.org/10.1016/j.expthermflusci.2009.03.004.

Levitsky, S.P. *et al.* (2005) "Water oxygenation in an experimental aerator with different air/water interaction patterns," *HAIT Journal of Science and Engineering B*, 2(1–2), pp. 242–253.

Li, H. *et al.* (2014) "Characteristics of micro-nano bubbles and potential application in groundwater bioremediation," *Water Environment Research*, 86(9), pp. 844–851. Available at: https://doi.org/10.2175/106143014X14062131177953.

Liew, K.C.S. *et al.* (2020) "Porous Venturi-orifice microbubble generator for oxygen dissolution in water," *Processes*, 8, pp. 1266–1280. Available at: https://doi.org/10.3390/pr8101266.

Loyless, J.C. and Malone, R.F. (1998) "Evaluation of air-lift pump capabilities for water delivery, aeration, and degasification for application to recirculating aquaculture systems," *Aquacultural Engineering*, 18, pp. 117–133.

Meng, H. *et al.* (2021) "The flow and mass transfer characteristics of concentric gas-liquid flow in an advanced static mixer," *Chemical Industry & Chemical Engineering Quarterly*, 27(1), pp. 57–68. Available at: https://doi.org/10.2298/CICEQ191213024M.

Oktaba, W. (1980) *Elementy statystyki matematycznej i metodyka doświadczalnictwa [Elements of Mathematical Statistics and Experimental Methodology]*. Warszawa: Państwowe Wydawnictwo Naukowe.

Puri, D., Sihag, P. and Thakur, M.S. (2023) "A review: Aeration efficiency of hydraulic structures in diffusing DO in water," *MethodsX*, 10, pp. 102092–102106. Available at: https://doi.org/10.1016/j.mex.2023.102092.

Putra, R.A. *et al.* (2019) "Comparison of gas–liquid flow characteristics in geometrically different swirl generating devices," *Energies*, 12(24), pp. 4653–4675. Available at: https://doi.org/10.3390/en12244653.

Revathi, D. *et al.* (2020) "Comparison of mixing hydrodynamics and mass transfer efficiency for a newly designed static mixer with different baffle elements," *International Journal of Scientific & Technology Research*, 9(4), pp. 1343–1348.

Sadatomi, M. *et al.* (2005) "Performance of a new micro-bubble generator with a spherical body in a flowing water tube," *Experimental Thermal and Fluid Science*, 29, pp. 615–623. Available at: https://doi.org/10.1016/j.expthermflusci.2004.08.006.

Sadatomi, M. *et al.* (2012) „Micro-bubble generation rate and bubble dissolution rate into water by a simple multi-fluid mixer with orifice and porous tube," *Experimental Thermal and Fluid Science*, 41, pp. 23–30. Available at: http://dx.doi.org/10.1016/j.expthermflusci.2012.03.002.

Sadatomi, M. *et al.* (2015) "Purification of deep water in a dam lake using micro-bubbles and/or eco-bio-ring," *International Journal of Environmental Science and Development*, 6(6), pp. 419–424. Available at: https://doi.org/10.7763/IJESD.2015.V6.629.

Suwartha, N. *et al.* (2020) "Effect of size variation on microbubble mass transfer coefficient in flotation and aeration processes," *Heliyon*, 6, pp. e03748–e03746. Available at: https://doi.org/10.1016/j.heliyon.2020.e03748.

Siwiec, T. and Morawski, D. (2000) "Eksperymentalne badania efektywności napowietrzania wody przy wykorzystaniu aeratorów rurowych [Experimental investigations of water aeration efficiency using pipe aerators]," *Gaz, Woda i Technika*, 1, pp. 23–27.

Świętochowski, K. *et al.* (2023) "Analysis of the use of a low-power photovoltaic system to power a water pumping station in a tourist town," *Energies*, 16, pp. 7435–7448. Available at: https://doi.org/10.3390/en16217435.

Talhaoui, A., Draoui, B. and Youcefi, A. (2021) "Effect of geometry design on mixing performance of Newtonian fluids using helical overlapped mixer elements in Kenics static mixer," *Journal of Applied Fluid Mechanics*, 14(6), pp. 1643–1656. Available at: https://doi.org/10.47176/jafm.14.06.32494.

Yadav, A., Kumar, A. and Sarkar, S. (2019) "Design characteristics of Venturi aeration system," *International Journal of Innovative Technology and Exploring Engineering*, 8(11), pp. 63–70. Available at: https://doi.org/10.35940/ijitee.J9929.0981119.

Yuan, F., Cui, Z. and Lin, J. (2020) "experimental and numerical study on flow resistance and bubble transport in a helical static mixer," *Energies*, 13, pp. 1228–1247. Available at: https://doi.org/10.3390/en13051228.